Biochemistry and Biophysics Reports 33 (2023) 101406

Contents lists available at ScienceDirect

Biochemistry and Biophysics Reports

journal homepage: www.elsevier.com/locate/bbrep

A dissected LMO2 functional analysis and clinical relevance in brain gliomas

Mei Yuan [a], Yanhong Yu [b], Yingying Meng [b], Huancheng Wu [c], Wei Sun [b,*]

[a] Department of Pharmacy, Beichen Hospitial, Tianjin, China
[b] School of Medicine, Nankai University, Tianjin, China
[c] Department of Neurosurgery, Beichen Hospitial, Tianjin, China

ARTICLE INFO

Keywords:
LMO2
Lower grade glioma
Glioblastoma
WGCNA
TCGA

ABSTRACT

Brain glioma is one of the cancer types with worst prognosis, and LMO2 has been reported to play oncogenic functions in brain gliomas. Herein, analysis of datasets from The Cancer Genome Atlas (TCGA) indicated that higher LMO2 level in patient samples indicated worse prognosis in lower grade gliomas (LGG) but not glioblastoma multiforme (GBM). Further, in tumor tissues consisting of a variety of cell types, LMO2 level indicated intratumoral endothelium and pattern recognition receptor (PRR) response in both LGGs and GBMs, and additionally indicated cytotoxic T-lymphocyte, M2 macrophage infiltration and fibroblast specifically in LGGs. Moreover, only in LGGs these aspects were significantly associated with patient survival, in either risky or protective manner, and these dissected associations can give a better prediction on patient prognosis than LMO2 alone. This study not only provided more detailed understandings of LMO2 functional representatives in brain gliomas but also demonstrated that dealing with certain gene (LMO2 in this study) in transcriptome data with the Weighted Gene Co-Expression Network Analysis (WGCNA) method was a robust strategy for dissecting exact and reasonable gene functions/associations in a complicated tumor environment.

1. Introduction

Brain glioma is one of the most malignant tumor types with generally poor prognosis. Based on the pathology, gliomas can be commonly classified as lower grade gliomas (LGGs) including astrocytoma, oligodendroglioma and oligoastrocytoma, and the even more aggressive glioblastoma multiforme (GBM). In general, gliomas consist of a mixture of cell types including not only tumor cells derived from neuroglial tissues but also blood vessels, infiltrated and resident immune cells, such as microglia. Histopathologically, gliomas are usually characterized by a lack of uniformity and boundaries, and may contain cysts, calcium deposits and focal areas of necrosis, and intracranial tumor cell spreading, metastasis and relapse are the major cause of patient death [1,2].

The *lmo2* (also known as *rbtn2* or *ttg2*) gene belongs to the LIM-domain-only (LMO) protein family, consists of only two tandem LIM-domains and plays absolutely as an adaptor that mediates protein-protein interactions [3]. LMO2 is initially expressed in hemangioblast, most highly expressed in hematopoietic cells and endothelium, and found to be essential through hematopoiesis and vascular development [4,5]. Pathologic function of LMO2 was initially associated with acute T lymphoblastic leukemia (T-ALL), for its capacity on T cell malignancy transformation [6,7], however, it is also found to be widely but lower expressed in kinds of epithelia and solid tumors [8,9]. Interestingly, LMO2 commonly showed decreased expression levels in majority of cancer types, with the exception in brain gliomas [9]. It has been reported that in brain gliomas, elevated LMO2 level showed oncogenic impact [10,11], and in TCGA glioma dataset, it can be observed that LMO2 is significantly higher expressed in GBM samples [9]. However, the LMO2 level represents a weighted average level from all types of cells intratumorally in the TCGA collected tumor samples, and the dissected LMO2 impacts in these tissues with mixed cell types remains largely unclear.

During the past decade, many efforts have been made to promote data-driven approaches for precision medicine in cancer research field including brain gliomas [12], including the usage of genetic multi-omics data, radiomics data, protein structure data and a variety of clinical data

Abbreviations: LMO2, LIM-Only-2; WGCNA, Weighted Gene Co-Expression Network Analysis; TCGA, The Cancer Genome Atlas; LGG, brain lower grade glioma; GBM, glioblastoma multiforme; PRR, pattern recognition receptor; CTL, cytotoxic T-lymphocyte.

* Corresponding author.
E-mail address: sunweibio@nankai.edu.cn (W. Sun).

https://doi.org/10.1016/j.bbrep.2022.101406
Received 3 October 2022; Received in revised form 1 December 2022; Accepted 6 December 2022

[13–16]. In this study, we aimed to address a full view of functional and clinical significance of the pivotal oncogenic gene LMO2 in gliomas primarily with a Weighted Gene Co-Expression Network Analysis (WGCNA) based bioinformatical strategy, and the results did give a well resolution of LMO2 functions in such complicated tumor environments.

2. Materials and methods

2.1. Study design

The flowchart of working pipeline for this study was described in Fig. 1. In brief, clinical information and LMO2 expression data of either glioblastoma multiforme (GBM) or lower grade glioma (LGG) in TCGA were used for survival and COX regression analysis, whilst transcriptome data together with LMO2 expression data were applied for WGCNA. Core LMO2-associated modules identified by WGCNA were annotated with their hubgenes, and core modules were further assessed with external datasets and applied for optimizing the COX regression models by substitution of LMO2.

2.2. Data collection

The mRNA and miRNA transcriptome datasets of glioblastoma multiforme (GBM) and lower grade glioma (LGG) in TCGA (Level 3), as well as their relevant clinical information files, were downloaded from the UCSC Cancer Genomics Browser (https://genome-cancer.ucsc.edu/). The RNA expression data matrix and clinical information were matched by sample ID for each sample. External transcriptome data from an independent study on brain medulloblastoma for assessment were downloaded from NCBI-GEO datasets (GSE143940 and GSE158413) [17].

2.3. Weighted gene Co-expression network analysis (WGCNA) and immune cell infiltration analysis

WGCNA was performed with R package "WGCNA" following the general pipeline. In brief, LMO2 expression level was applied to calculate the correlations with all other genes for constructing the gene co-expression network in LGG or GBM. The hub genes of each module were selected with the criteria of >0.8 of module membership (MM) values and <0.05 of p-values of the correlation coefficients with LMO2, and the cutoff value of topological overlap measure (TOM) was initially set as 0.2 and adjusted dynamically. Network plots of core genes of each module were drawn by cytoscape_3.7.2. Immune cell infiltration analysis was performed with the R package "Cibersort" following the default pipeline. Relative plots and statistics were dealt with R software.

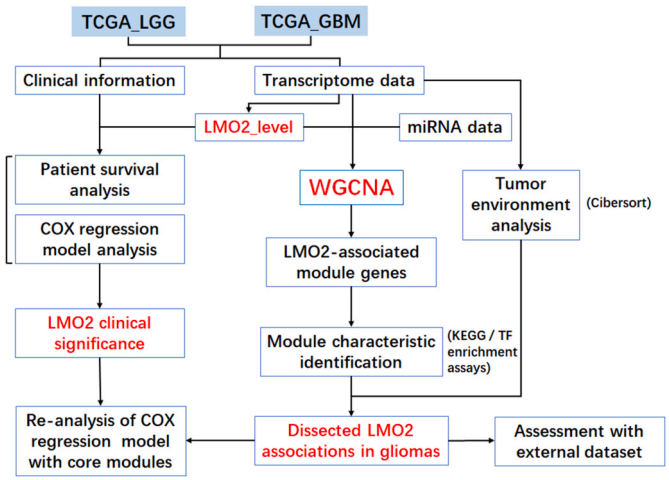

Fig. 1. The flowchart of working pipeline for this study.

2.4. COX regression model and survival analysis

The clinical and survival data of LGG and GBM in TCGA were downloaded as above mentioned. The COX regression and survival analysis were performed with R package "survival", and the COX regression model evaluation was performed with R package "pec".

2.5. Gene function enrichment analysis

The KEGG and transcriptional factor (TF) enrichment assay were performed with R package "ClusterProfiler" [18]. The datasets of transcriptional factor (TF) and miRNA target profiles were downloaded from GSEA website (http://www.gsea-msigdb.org/). All images were drawn by R software.

3. Results

3.1. LMO2 is a risk factor for patient survival in lower grade brain gliomas but not in glioblastoma multiforme

In TCGA datasets, glioblastoma multiforme (GBM) samples expressed significantly higher levels of LMO2 than brain lower grade glioma (LGG) samples and normal tissues (Fig. 2A), and as expected, GBM patients had prominent worse prognosis than LGG patients (Fig. S1A). Further, all LGG or GBM samples were divided into LMO2-high and LMO2-low patient groups by the median LMO2 level, respectively, and it could be observed that in LGGs, LMO2- high patients had significantly worse prognosis (shorter survival) whereas in GBM, LMO2 had no discriminating effect on patient survival (Fig. 2B and C). In addition, COX regression models incorporating LMO2 level and other general clinical information, including patients age, gender, race and intermediate tumor dimension at diagnosis, suggested that LMO2 level was the most risky factor specifically in LGGs (hazard ratio: 2.01, $p < 0.001$), while the rest clinical factors had rather limited impacts in either LGGs or GBMs, although the intermediate tumor dimension at diagnosis was inclined to be a protective factor in LGGs (Fig. 2D and E).

3.2. LMO2 is highly associated with endothelia, fibroblasts, cytotoxic T-lymphocytes, macrophages and pattern recognition receptor responses in LGGs

Since that LMO2 was a risk factor specifically for LGG, we next aimed to resolve the functional associations of LMO2 in detail. Weighted Gene Co-Expression Network Analysis (WGCNA) on LGG mRNA transcriptome data (Fig. S1B) suggested 5 modules with high associations with LMO2 level (the grey60, lightcyan, lightyellow, lightgreen and brown module, Fig. 3A). Among these modules, the grey60 and lightcyan module showed the closest relations with LMO2 while the other three were relatively distant (Fig. 3B). Hubgenes of each module were screened out with the criteria of >0.3 of correlation coefficients with LMO2 level and >0.8 of correlation coefficients with the module membership (MM) score (Fig. S1C). Notably, the central hubgenes CDH5 (VE-Cadherin), MMRN2 and NOS3 (eNOS) in the lightcyan module indicated that this module represented the markers of endothelium. Similarly, the lightgreen module characterized by the central genes of CD2, CD3, LCK and GZMA/K represented the cytotoxic T-lymphocytes (CTLs), the brown module characterized by the central genes of FCGR1A (CD64), CSF1R and LILRB4 represented the macrophages (probably anti-inflammatory macrophages (M2) or tumor-associated macrophages (TAMs) because of LILRB4 expression), the grey60 module characterized by the central genes of collagens and LUM (Lumican) represented the fibroblasts, and the lightyellow module consisted of two parts, the MHC-I antigen presenting genes characterized by HLA-B and the others characterized as the down-stream genes of pattern recognition receptor (PRR) signaling pathways (Fig. 3C). Moreover, enrichment assay of genes in each module on transcriptional factors (TFs) indicated that

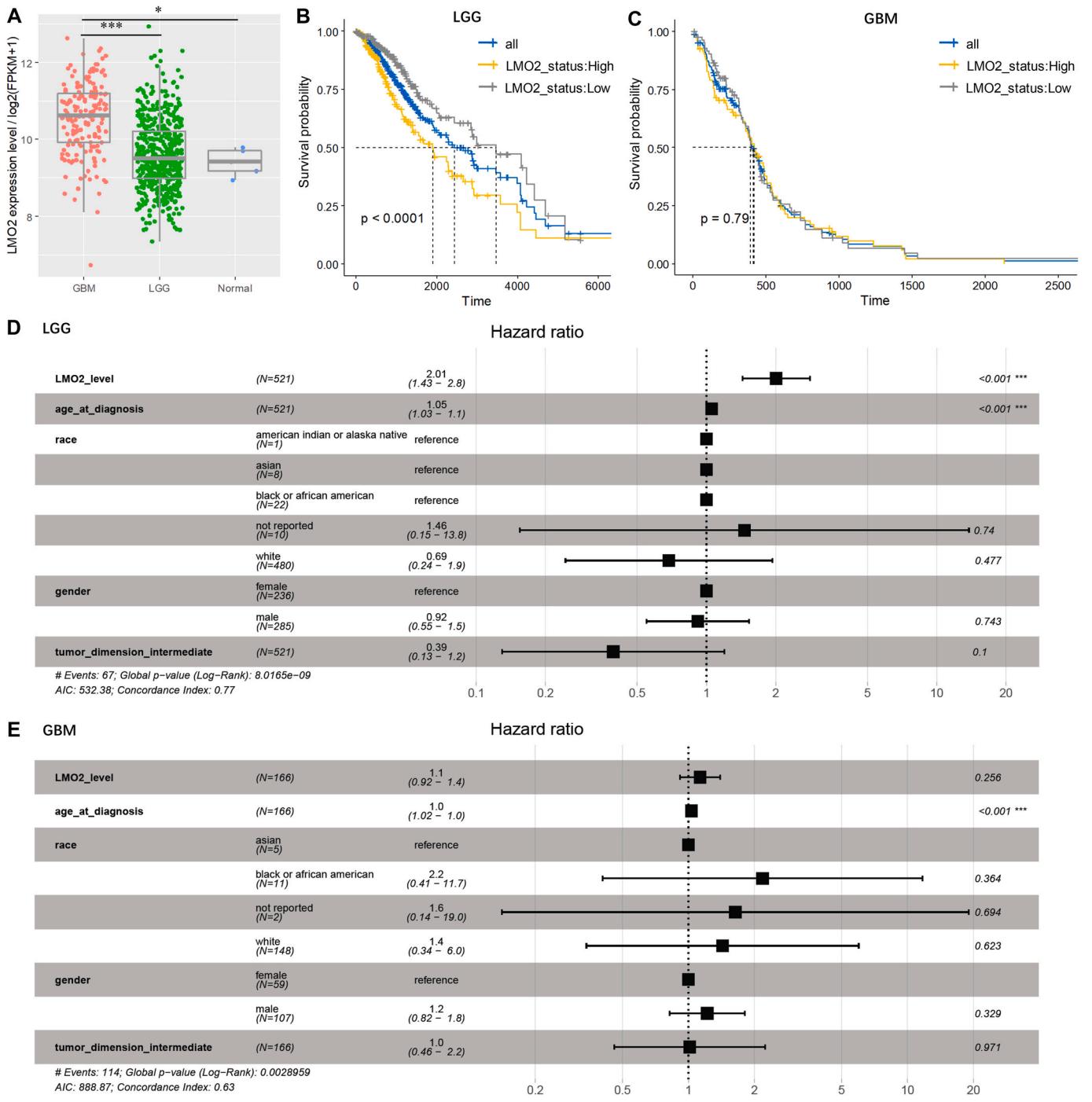

Fig. 2. LMO2 is a risk factor for patient survival in lower grade brain gliomas but not in glioblastoma multiforme. (A) A dotplot combined with boxplot showing the distribution of LMO2 expression level in GBMs, LGGs and brain normal tissues from TCGA datasets. *, TukeyHSD test, $p < 0.05$; ***, $p < 0.001$. **(B–C)** Kaplan-Meier Curves of LGG patients (B) or GBM patients (C) from TCGA grouped by the median of LMO2 expression level in the dataset. Relative information was marked on the plot. **(D–E)** Forest plots showing the results of COX regression model analysis of LGGs (D) and GBMs (E) consisting of LMO2 level, age at diagnosis, gender, race and intermediate tumor diameters as the variables. Relative information was listed in the tables.

hubgenes in endothelial module were specifically enriched on ETS2, NERF (ELF2), GATA and LMO2 complex profiles, all of which were known intrinsic LMO2 transcriptional regulating targets in endothelia; the hubgenes in PRR response module were particularly enriched on the profiles of IRFs, which were the key responding TFs to PRRs, and the hubgenes in macrophage module were enriched on some typical myeloid TFs including ETS family, AML1/CBF and MAML1/NOTCH1 (Fig. 3D). On the other hand, function (KEGG) enrichment assay indicated that the fibroblast module genes were primarily enriched on PI3K-AKT pathway and extracellular matrix/focal adhesion functions, the endothelial module genes were primarily enriched on PI3K-AKT, MAPK, Calcium signaling pathways as well as cell adhesion functions, the MHC-I antigen presentation/PRR responding module genes were specifically enriched on damage-associated molecular pattern (DAMP) signaling pathways, including NOD-like, RIG-like and Toll-like signaling, and the macrophage module genes were relatively weaker enriched on some of the above mentioned functions and additional TNF signaling, apoptosis and necroptosis (Fig. 3E). These integrated data were largely accordance

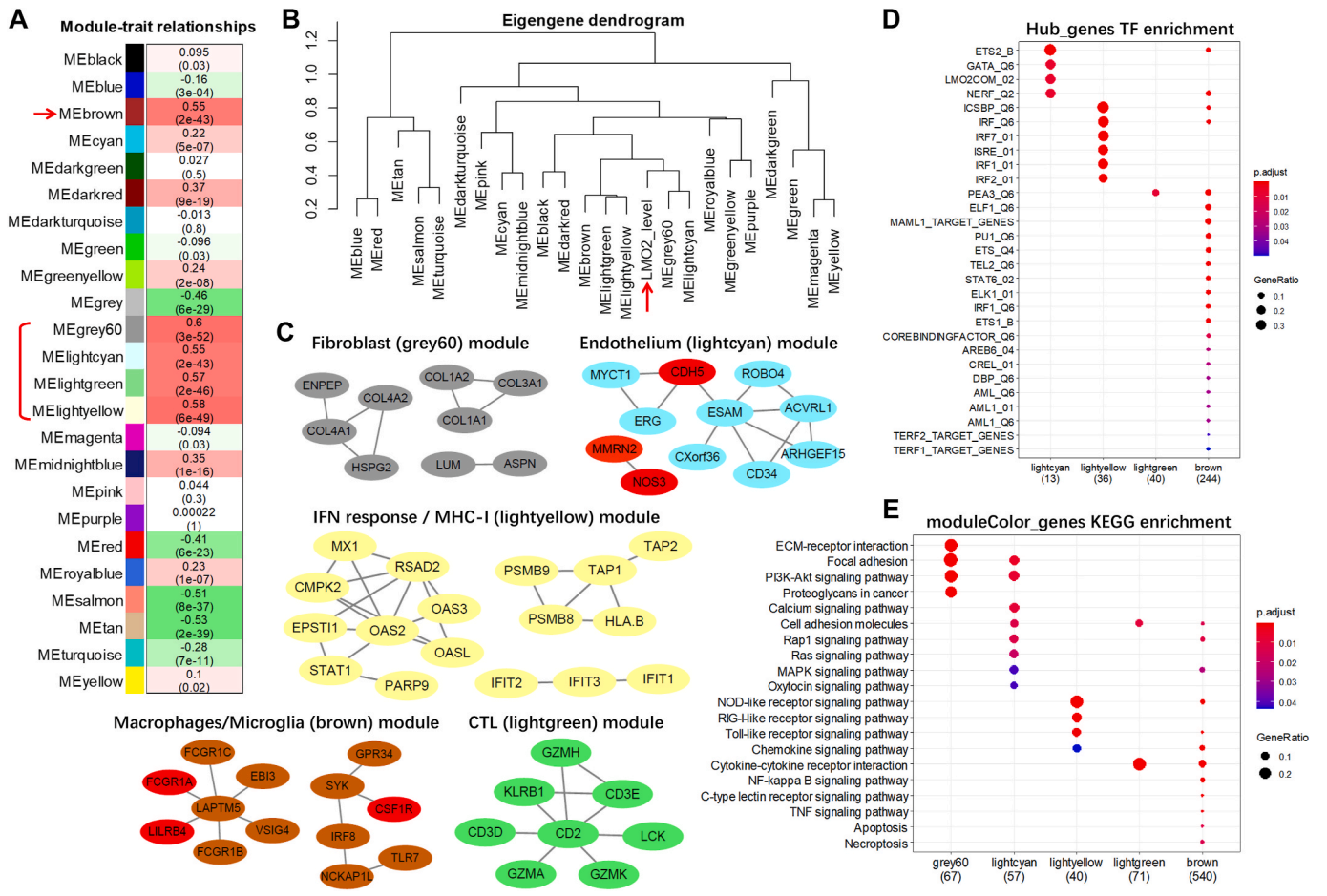

Fig. 3. LMO2 is highly associated with endothelia, fibroblasts, cytotoxic T-lymphocytes, macrophages and pattern recognition receptor responses in LGGs. (A) A heatplot showing the correlations of LMO2 and each module identified by WGCNA algorithm. Correlation coefficients and *p*-values between LMO2 and each module were marked on the plot, and the most significantly related modules were indicated by red arrow or bracket. **(B)** The epigengene dendrogram showing the cluster distance of LMO2 and other modules. The LMO2 position was indicated by red arrow. **(C)** The plots of hubgenes network of each LMO2 most-related module. Module information was marked on each plot and the key marker genes in each module that indicated the module representative/characteristic were marked in red. **(D)** The dotplot showing the result of enrichment assay on transcriptional factor (TF) profiles of hub genes in each module as marked on the plot. **(E)** The dotplot showing the result of KEGG enrichment assay of all genes in each module as marked on the plot. Other relative information was marked in the legends of the plots. (For interpretation of the references to colour in this figure legend, the reader is referred to the Web version of this article.)

with the intrinsically molecular characteristic of each type of cell dissected by WGCNA, and further supported that the incorporation of fibroblasts, endothelia, CTLs, macrophages in tumor tissues and MHC-I antigen presenting/activation of damage-associated molecular pattern signaling driven by tumor cells were the major LMO2 associations in LGGs.

In glioblastoma multiforme (GBM), WGCNA with the same strategy as in LGG (Figs. S1D and E) suggested 3 modules with only moderate correlations with LMO2 level (the paleturquoise, darkred and darkorange module, Fig. S2A), with the paleturquoise and darkred module showing relatively closer relations with LMO2 in the dendrogram (Fig. S2B). Of note, both the paleturquoise and darkred module represented the endothelia characterized by ESAM, MMRN2 and TIE1, and the darkorange module represented the PRR responses (Fig. S2C). Accordingly, TF enrichment assays indicated that the hubgenes of endothelial and PRR response modules were primarily enriched on ETS/GATA/E47 and IRF target profiles respectively (Fig. S2D), and functional enrichment assay indicated that endothelial module genes were enriched on PI3K-AKT, MAPK, Calcium signaling pathways and focal adhesion functions while the PRR responding module genes were enriched on NOD-like, RIG-I-like, Toll-like, C-type lectin signaling pathways, as well as necroptosis (Fig. S2E). These LMO2 associations were largely identical with LGGs, but in GBMs LMO2 lacked prominent associations with fibroblast, CTL or macrophage incorporation in tumor tissues.

3.3. *Other features of LMO2 associations with immune cells and microRNAs in LGGs*

Using the CIBERSORT algorithm, we further explored the overall feature of infiltrated immune cells based on mRNA transcriptome data in all brain samples from TCGA. The results revealed that M2 macrophage (anti-inflammatory macrophage/TAM) was the major component of infiltrated immune cells in both LGGs and GBMs, and in GBMs there were also relatively higher ratios of M0 macrophages (unstimulated macrophages). However, CD8 T-cell (cytotoxic T-lymphocyte, CTL) proportion was rather low in both LGGs and GBMs (Fig. 4A), although this group of cells were significantly associated with LMO2 level in LGGs. These were further supported by the commonly high expression of central hubgenes in macrophage module (the brown module) and relatively low level of central hubgenes in CTL module (the lightgreen module) previously identified (Fig. S3A). Additionally, LMO2 showed significantly positive correlation with the ratio of M2 macrophages in LGGs but not in GBMs (Fig. 4B), and for M0 macrophage, although some rich in GBMs, no significant correlation with LMO2 was observed (Fig. S3B). For CD8 T-cells, weakly positive correlation with LMO2 in

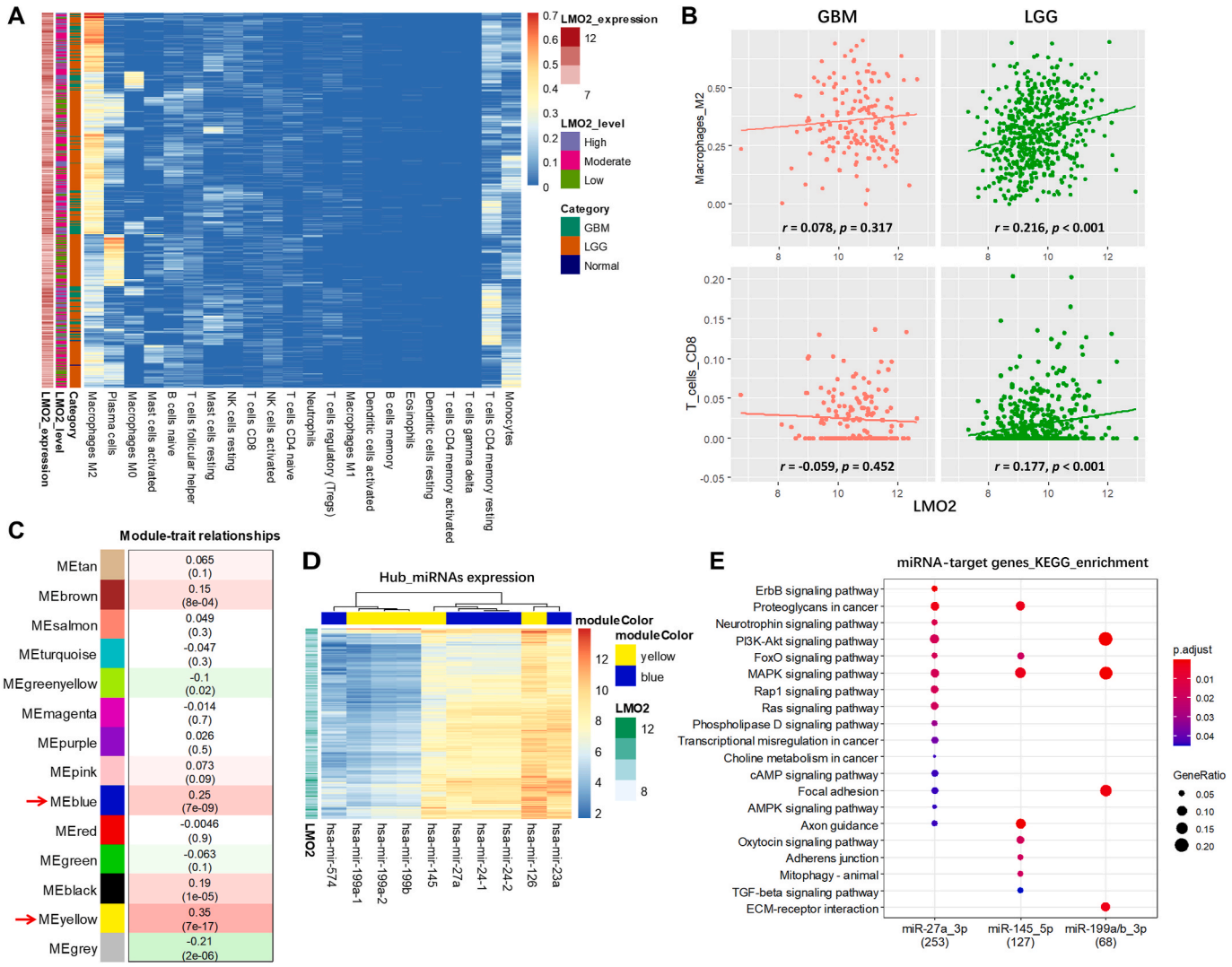

Fig. 4. The associations of LMO2 with immune features and microRNAs in LGGs. (A) A heatmap showing the relative abundance of infiltrated kinds of immune cells in TCGA brain glioma samples given by Cibersort algorithm. The LMO2 expression value (given as log2(FPKM+1)), LMO2 level category and sample category of each sample were marked on the plot. **(B)** Dotplots showing the distribution of LMO2 level versus M2 macrophage percentage (up) or $CD8^+$ T cell percentage (down) of each sample in TCGA dataset. The trendlines, correlation coefficients (r) and p-values were marked on the plots. **(C)** Heatplot showing the correlations of LMO2 and each module identified by WGCNA algorithm in miRNA dataset in LGGs. Correlation coefficients and *p*-values between LMO2 and each module were marked on the plot, and the most significantly related modules were indicated by red arrows. **(D)** Heatmap showing the expression level of hub miRNAs identified in the blue and yellow modules. Data were given as log2 (TPM+1) and other relative information was marked on the plot. **(E)** The dotplot showing the result of KEGG enrichment assay of relative miRNA target genes as marked on the plot. Relative information was marked in the legends of the plots. (For interpretation of the references to colour in this figure legend, the reader is referred to the Web version of this article.)

LGGs was detected as well and no correlation was observed in GBMs either (Fig. 4B).

In addition, since that most of the functional associations of LMO2 were observed in LGGs, the feature of correlations between LMO2 and microRNAs (miRNAs), which may represent the minor effect of LMO2 in post-transcriptional level, were further explored in LGGs as well. First, based on the expression level, 300 miRNAs with effective expression were selected for the following analysis (Fig. S3C). WGCNA on those miRNAs (Fig. S3D) suggested 2 modules with moderate-to-low correlations with LMO2 level (the yellow and blue module, Fig. 4C), however, neither of them showed close correlation with LMO2 in the dendrogram (Fig. S3E). Under the criteria of >0.2 of correlation coefficients with LMO2 level and >0.8 of correlation coefficients with the module membership score (Fig. S3F), miR-23a, miR-24-1, miR-24-2, miR-27a and miR-574 were screened out as the hub-miRNAs in blue module, and miR-126, miR-145, miR-199a-1, miR-199a-2 and miR-199b were screened out as the hub miRNAs in yellow module. Among these miRNAs, miR-574, miR-199a-1, miR-199a-2 and miR-199b were relatively less expressed (Fig. 4D). Of note, all hub-miRNAs of the yellow module are reported to be highly endothelium-associated as well [19–22], thus they further indicated the associated between LMO2 and endothelia. Accordingly, target genes of these miRNAs were matched based on the miRNA targets database from GSEA (http://www.gsea-msigdb.org/gsea/), and the low expressed target genes were excluded for following analysis (Fig. S3G). KEGG enrichment assay indicated that enriched terms were restricted to the target gene sets of miR-27a-3p, miR-145–5p and miR-199a/b-3p. Further, the miR-145–5p and miR-199a/b-3p target profiles were primarily enriched on similar signaling pathways that were also enriched by endothelium module genes, including RAS-MAPK, PI3K-AKT and focal adhesion functions, whilst the miR-27a-3p target profiles could additionally enriched on some cancer related pathways (Fig. 3E), probably for that miR-27a-3p was reported to be tumor-associated but exhibit dual-directional functions on either tumor progression or tumor inhibition in different types

of cancers [23,24].

3.4. Incorporation of the integrated WGCNA modules in COX regression model gave a better prognostic prediction than using LMO2 level alone in LGG

Prominent correlation of LMO2 with endothelium and PRR response

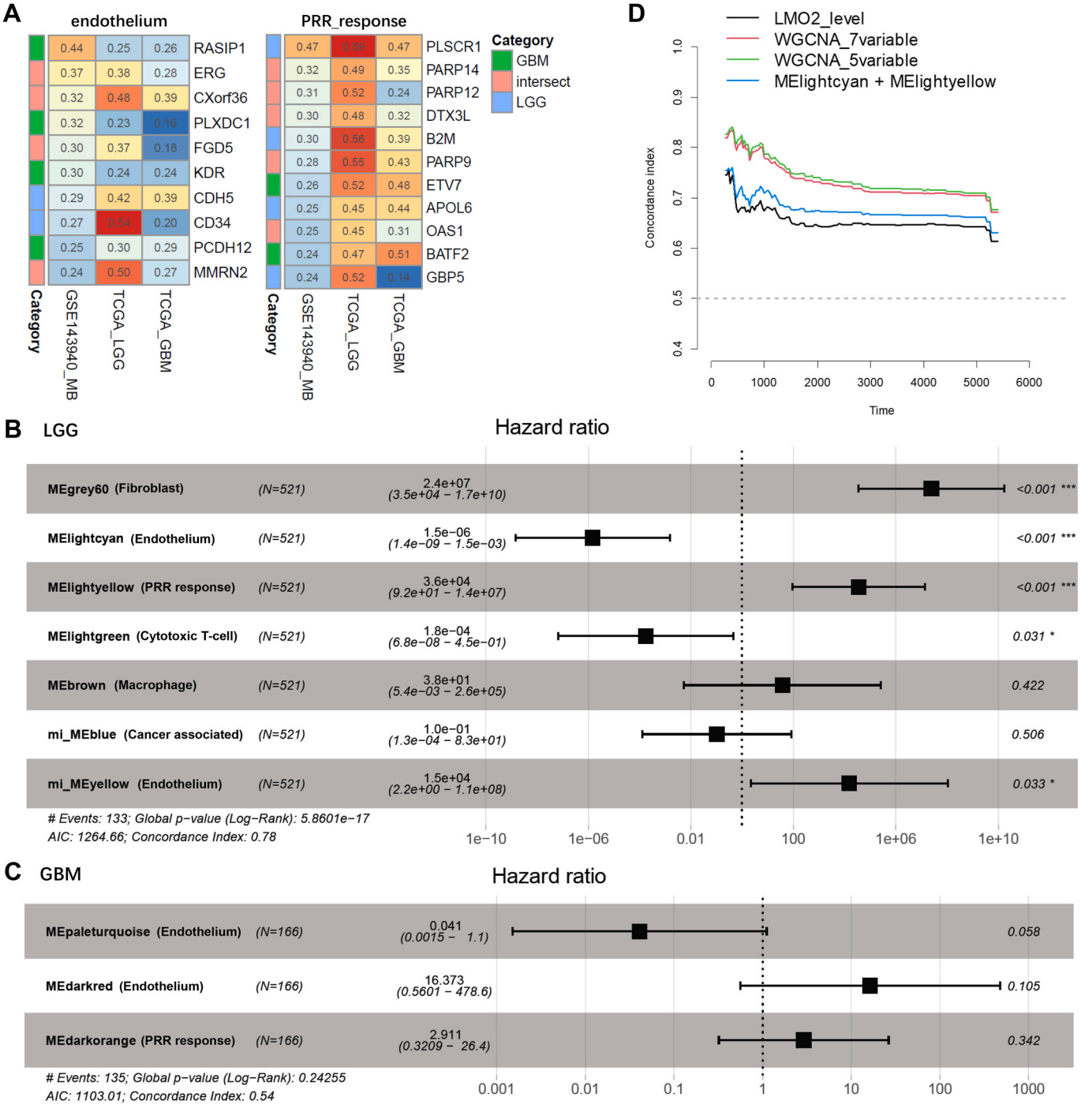

Fig. 5. Incorporation of the integrated WGCNA modules in COX regression model gave a better prognostic prediction than using LMO2 level alone in LGG. **(A)** heatplots showing the correlation coefficients of LMO2 with core hubgenes in endothelium and PRR response modules in TCGA-LGG, TCGA-GBM and TCGA-independent medulloblastoma (MB) datasets. All selected genes in the plots were statistically significantly correlated with LMO2 ($p < 0.05$) in MB, and the category in the legend indicated that relative genes were also identified in LGG, GBM or both (intersect). **(B–C)** Forest plots showing the results of COX regression model analysis of LGGs (B) and GBMs (C) consisting of the LMO2 mostly associated modules identified as the variables, respectively. Relative information was listed in tables. **(D)** The plot giving the comparison of the COX regression models consisting of different combinations of variables. The combinations of variables were given in the legends. WGCNA_5 variable model included the grey60, lightcyan, lightgreen, lightyellow module from transcriptome data and yellow module from miRNA data, and WGCNA_7 variable model additionally included the brown module from transcriptome data and the blue module from miRNA data. (For interpretation of the references to colour in this figure legend, the reader is referred to the Web version of this article.)

had been commonly observed in both LGG and GBM datasets from TCGA, in addition, in the independent datasets from a study of brain medulloblastoma, the core marker genes of these two modules, such as ERG and MMRN2 in endothelium and OAS1, PARPs and DTX3L in PRR response, were significantly correlated with LMO2 as well (Fig. 5A), further supporting the above-mentioned common associations of LMO2 in brain gliomas. Finally, we used the previously identified, LMO2 mostly correlated WGCNA modules to replace LMO2 itself and rebuild the COX regression models in LGG and GBM patient samples, respectively. As shown in Fig. 5B, in LGGs, the grey60 (fibroblast), lightcyan (endothelium), lightgreen (CTL), lightyellow (PRR response) module from mRNA transcriptome data and the yellow (endothelium) module from miRNA transcriptome data showed statistically significant impact on patient survival. Moreover, the CTL and endothelium module showed protective effect, while the fibroblast, MHC-I antigen presenting/PRR response module and miRNA endothelium module showed risky impact in the model. In contrast in GBM, none of the paleturquoise, darkred (representing endothelium) or darkorange (representing the PRR response) module had any significant impacts in the COX regression model (Fig. 5C). Finally, for LGG patients, the WGCNA-5 variable COX model using all significant modules (the grey60, lightcyan, lightgreen, lightyellow and yellow module) had the highest prognostic prediction accuracy (concordance index 70%–80%) comparing with models using LMO2 alone (concordance index 65%–75%) or any other combination of the module variables (Fig. 5D).

4. Discussion

Although LMO2 has been found to be ubiquitously expressed in kinds of solid tumors [8,9], it has extraordinary expression patterns in different cell types. In brain tumor environment, it is most highly expressed in endothelia as a pivotal transcriptional regulator, moderately expressed in myeloid cells (macrophages) and non-expressed in T and NK cells [3,5]. In this study, based on the transcriptome data from brain tumor tissues, which means that they contain at least tumor cells, stroma cells, endothelia and immune cells, we dissected several LMO2 functional associations in both brain lower grade glioma (LGG) and glioblastoma multiforme (GBM), including core associations with fibroblasts, endothelia, macrophages, cytotoxic T-lymphocytes and MHC-I antigen presenting/pattern recognition receptor (PRR) responses in LGGs, and primary associations with endothelia and PRR responses in GBMs.

In LGGs, although the overall effect of LMO2 was a risk factor for patient prognosis, its dissected associations had divergent impacts: the LMO2-associated fibroblast, MHC-I antigen presenting/PRR responses and endothelium-related miRNAs were risk factors whereas LMO2-associated endothelia and CTLs were protective factors. Notably, the endothelium and fibroblast modules were closely associated and it seemed that they together represented the intratumoral angiogenesis status, and their impacts on prognosis were largely neutralized by each other. Correspondingly, endothelium module identified in GBMs did not show any prominent impact on prognosis either. Another observation was that both endothelium-related genes and miRNAs were positively correlated with LMO2, but they showed completely inverse impact in the COX model. This should be due to that microRNAs were intrinsically negative regulators for their target gene expression in post-transcriptional level, and the target genes of relative miRNAs were largely involved in endothelial functions. Moreover, no matter in LGGs or GBMs, the LMO2-associated endothelial module genes were particularly enriched on LMO2 regulating transcriptional factors (ETS, GATA and LMO2 complex) and endothelium-related signaling pathways (PI3K-AKT, MAPK, Calcium signaling pathways and cell adhesion functions), suggesting that LMO2 itself could be considered as an indicator of intratumoral endothelia abundance, although this may not correlate to patient prognosis in neither LGGs nor GBMs.

The PRR response was another common LMO2-associated module in both LGGs and GBMs. In tumor environment, the PRR response is primarily derived from the damage-associated molecular pattern (DAMP) signaling (eg. NOD-like signaling), which was largely initiated by tumor cell death and content release, and executed by innate immune cells such as macrophages, as well as tumor cell themselves. The common consequence of PRR response included apoptosis, pyroptosis and necroptosis of tumor cells, and the latter two generally led to inflammation, more PRR stimuli release and boosted DAMP response in the tumor environment [25]. However, although the DAMP response should apparently play anti-tumor effect, the LMO2 associated PRR response showed prominently adverse impact on patient survival in LGGs, probably depending on other physiopathologic consequences of these PRR responding events. Moreover, LMO2 level did correlate with macrophage/resident microglia, particularly the M2 macrophage infiltration in LGGs, but this group of cells themselves seemed not contributing much for patient prognosis either.

Meanwhile, the MHC-I antigen presenting function, which was identified in the same module with PRR response and prominently associated with LMO2 in LGGs as well, was closely related to the crosstalk with cytotoxic T-lymphocytes (CTLs). Notably, a prominent association of LMO2 and CTL module was indeed observed in LGGs, and this module showed protective effect in the COX model of LGG. LMO2 is not expressed in any subtypes of T cells, thus the association of LMO2 and this module could indicate the effect of LMO2 on enhancing CTL infiltration and cytotoxicity in tumor environment.

Till now, a variety of approaches have been developed for characteristic identification and precision medicine in gliomas, such as using integrated genetic multi-omics and radiomics data [13,14]. In this study, we aimed to apply a WGCNA-based strategy to investigate the functional aspects of certain genes (LMO2 in this study) from transcriptome data in a complicated glioma environment, and the results confirmed that the LMO2 functional associations had been indeed dissected into several aspects exactly and reasonably in brain gliomas, including common endothelium and pattern recognition receptor (PRR) response and LGG-specific cytotoxic T-lymphocyte (CTL) infiltration. Thus, this study not only provided more details for the understanding of LMO2 function aspects in brain gliomas but also demonstrated that the WGCNA-based approach was a robust tool for dissecting certain gene functions/associations in a mixed tumor environment.

Author contributions

YM: analysis and interpretation of data; YYH and MYY: part of WGCNA work; WHC: revising the article critically for important intellectual content; SW: the conception and design of the study, and final approval of the version to be submitted.

Declaration of competing interest

There is no conflict of interest in this study.

Data availability

Data were downloaded from the UCSC Cancer Genomics Browser (https://genome-cancer.ucsc.edu/) and NCBI-GEO DataSets (https://www.ncbi.nlm.nih.gov/gds/)

Acknowledgement

This work is supported by the National Natural Science Foundation of China General Programs (No. 81772976).

Appendix A. Supplementary data

Supplementary data to this article can be found online at https://doi.org/10.1016/j.bbrep.2022.101406.

References

[1] V.P. Collins, Brenner's Encyclopedia of Genetics, second ed., Gliomas, 2013, pp. 334–336.
[2] M. Beatriz, S. Lopes, S. VandenBerg, Diagnostic histopathology of tumors, Chapter 26 (2021) 2067–2171.
[3] J. Chambers, T.H. Rabbitts, LMO2 at 25 years: a paradigm of chromosomal translocation proteins, Open biology 5 (2015), 150062.
[4] Y. Yamada, A.J. Warren, C. Dobson, et al., The T cell leukemia LIM protein Lmo2 is necessary for adult mouse hematopoiesis, Proc. Natl. Acad. Sci. U.S.A. 95 (1998) 3890–3895.
[5] K. Pike-Overzet, D. de Ridder, F. Weerkamp, et al., Ectopic retroviral expression of LMO2, but not IL2Rc, blocks human T-cell development, Leukemia 21 (2007) 754–763.
[6] M.P. McCormack, L.F. Young, S. Vasudevan, et al., The Lmo2 oncogene initiates leukemia in mice by inducing thymocyte self-renewal, Science 327 (2010) 879–883.
[7] S. Hacein-Bey-Abina, C. Von Kalle, M. Schmidt, et al., LMO2-associated clonal T cell proliferation in two patients after gene therapy for SCID-X, Science 302 (2003) 415–419.
[8] C. Agostinelli, J.C. Paterson, R. Gupta, et al., Detection of LIM domain only 2 (LMO2) in normal human tissues and haematopoietic and non-haematopoietic tumours using a newly developed rabbit monoclonal antibody, Histopathology 61 (2012) 33–46.
[9] Y. Liu, D. Huang, Z. Wang, et al., LMO2 attenuates tumor growth by targeting the Wnt signaling pathway in breast and colorectal cancer, Sci. Rep. 6 (2016), 36050.
[10] S.H. Kim, E.J. Kim, M. Hitomi, et al., The LIM-only transcription factor LMO2 determines tumorigenic and angiogenic traits in glioma stem cells, Cell Death Differ. 22 (2015) 1517–1525.
[11] C.G. Park, S.H. Choi, S.Y. Lee, et al., Cytoplasmic LMO2-LDB1 complex activates STAT3 signaling through interaction with gp130-JAK in glioma stem cells, Cells 11 (2022) 2031.
[12] N. Wijethilake, D. Meedeniya, C. Chitraranjan, et al., Glioma survival analysis empowered with data engineering—a survey, IEEE Access, 9(2021), 43168-43191.
[13] N. Wijethilake, D. Meedeniya, C. Chitraranjan, et al., Survival Prediction and Risk Estimation of Glioma Patients Using mRNA Expressions, arXiv:2011.00659v1 [q-bio.GN].
[14] N. Wijethilake, M. Islam, D. Meedeniya, et al., Radiogenomics of Glioblastoma: Identification of Radiomics Associated with Molecular Subtypes. arXiv: 2010.14068v1 [q-bio.QM].
[15] A.V. Popov, A.V. Endutkin, D.D. Yatsenko, et al., Molecular dynamics approach to identification of new OGG1 cancer-associated somatic variants with impaired activity, J. Biol. Chem. 296 (2021), 100229.
[16] S.I. Allec, Y. Sun, J. Sun, et al., Heterogeneous CPU+GPU-Enabled simulations for DFTB molecular dynamics of large chemical and biological systems, J. Chem. Theor. Comput. 15 (2019) 2807–2815.
[17] K.S. Wu, T.Y. Jian, S.Y. Sung, et al., Enrichment of tumor-infiltrating B cells in group 4 medulloblastoma in children, Int. J. Mol. Sci. 23 (2022) 5287.
[18] G. Yu, L.G. Wang, Y. Han, et al., clusterProfiler: an R package for comparing biological themes among gene clusters, OMICS A J. Integr. Biol. 16 (2012) 284–287.
[19] S. Wang, A.B. Aurora, B.A. Johnson, et al., The endothelial-specific microRNA miR-126 governs vascular integrity and angiogenesis, Dev. Cell 15 (2008) 261–271.
[20] K.R. Cordes, N.T. Sheehy, M.P. White, et al., miR-145 and miR-143 regulate smooth muscle cell fate and plasticity, Nature 460 (2009) 705–710.
[21] S. Yamaguchi, K. Yamahara, K. Homma, et al., The role of microRNA-145 in human embryonic stem cell differentiation into vascular cells, Atherosclerosis 219 (2011) 468–474.
[22] A. Hashemi Gheinani, F.C. Burkhard, H. Rehrauer, et al., MicroRNA MiR-199a-5p regulates smooth muscle cell proliferation and morphology by targeting WNT2 signaling pathway, J. Biol. Chem. 290 (2015) 7067–7086.
[23] X. Li, M. Xu, L. Ding, et al., MiR-27a: a novel biomarker and potential therapeutic target in tumors, J. Cancer 10 (2019) 2836–2848.
[24] J. Zhang, Z. Cao, G. Yang, et al., MicroRNA-27a (miR-27a) in solid tumors: a review based on mechanisms and clinical observations, Front. Oncol. 9 (2019) 893.
[25] D.V. Krysko, A.D. Garg, A. Kaczmarek, et al., Immunogenic cell death and DAMPs in cancer therapy, Nat. Rev. Cancer 12 (2012) 860–875.